

DocMAE: Document Image Rectification via Self-supervised Representation Learning

Shaokai Liu[†]

University of Science and Technology
of China
Hefei, China
liushaokai@mail.ustc.edu.cn

Hao Feng[†]

University of Science and Technology
of China
Hefei, China
haof@mail.ustc.edu.cn

Wengang Zhou

University of Science and Technology
of China
Hefei, China
zhwg@ustc.edu.cn

Houqiang Li

University of Science and Technology of China
Hefei, China
lihq@ustc.edu.cn

Cong Liu

iFLYTEK Research
Hefei, China
congliu2@iflytek.com

Feng Wu

University of Science and Technology of China
Hefei, China
fengwu@ustc.edu.cn

Abstract—Tremendous efforts have been made on document image rectification, but how to learn effective representation of such distorted images is still under-explored. In this paper, we present DocMAE, a novel self-supervised framework for document image rectification. Our motivation is to encode the structural cues in document images by leveraging masked auto-encoder to benefit the rectification, *i.e.*, the document boundaries, and text lines. Specifically, we first mask random patches of the background-excluded document images and then reconstruct the missing pixels. With such a self-supervised learning approach, the network is encouraged to learn the intrinsic structure of deformed documents by restoring document boundaries and missing text lines. Transfer performance in the downstream rectification task validates the effectiveness of our method. Extensive experiments are conducted to demonstrate the effectiveness of our method.

Index Terms—Document Image Rectification, Self-supervised Representation Learning, Transformer

I. INTRODUCTION

With the ubiquitous accessibility of smartphones, document digitization becomes much more convenient than before. However, document images captured by smartphones usually suffer from various distortions, due to some stochastic factors, such as sheet deformations, camera angles, and scene illuminations. They bring difficulties to the downstream visual tasks, such as automatic text recognition [1], content analysis [2], and question answering [3]. To overcome these issues, document image rectification has been actively studied in the past decades.

Traditional solutions [4]–[9] to document image rectification are usually based on 3D reconstruction techniques. These methods either resort to extra hardware or register multi-view images to reconstruct a 3D shape of the deformed document, which inevitably brings lots of inconveniences so as to block their further real applications. Recently, learning-based methods [10]–[15] estimate a dense flow field from the distorted image to the distortion-free one, which have shown promising

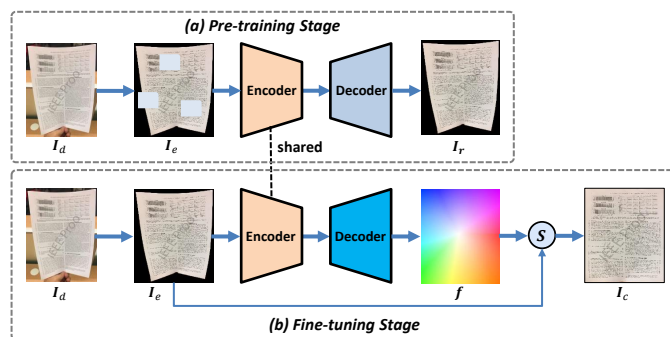


Fig. 1. An overview of our DocMAE. It consists of two stages: (a) A pre-training stage that reconstructs the randomly masked patches; (b) A fine-tuning stage that transfers the learned representations for distortion rectification. “ S ” denotes the warping operation based on bilinear sampling.

performance. With the flow field, the input distorted image can be unwarped for rectification. Although these methods report superior performance, how to learn effective representations of a distorted document image is still under-explored.

In document image rectification, it is crucial to extract the structural information of the deformed document. In a document image, the most informative cues for rectification exist in the document boundaries and text lines. Concretely, the document boundaries contain information about the global physical deformation and shooting angles, while the text lines show the deformation of local regions. Besides, there is an explicit prior on the text lines that the distorted horizontal text lines are straight in the rectified image. To obtain the structure representation, traditional methods resort to auxiliary hardware [4]–[6], [16] or multi-view images [7], [8], [17]. Recently, learning-based method [15] have learnt a 3D coordinate map with a U-Net [18]. However, these existing structure representation learning methods for document images require auxiliary hardware or human supervision.

To avoid the inconvenience of existing structure representa-

[†] The first two authors contribute equal to this work.

This work is supported by the Strategic Priority Research Program of Chinese Academy of Sciences under Grant No. XDC08030000.

tion methods, we propose DocMAE, a self-supervised learning-based framework for document image rectification, inspired by the success of MAE [19]. The framework of our DocMAE is simple, which consists of a pre-training stage for distortion representation learning and a fine-tuning stage for distortion rectification. Technically, during the pre-training stage, we first mask the random patches of the background-excluded document images and then reconstruct the missing pixels. Note that here the reconstruction is conducted on the background-excluded document images to avoid non-unique solutions because a document can be placed in various scenes. Besides, to support pre-training process, we collect a large-scale synthetic document distortion dataset named LDIR, which fully simulates the various distortion of real document images. Then, in fine-tuning stage, the learned representations are transferred to the downstream rectification task.

Extensive experiments are conducted on our proposed LDIR dataset, Doc3D dataset [15], and DocUNet benchmark dataset [10]. The results verify the effectiveness of our method as well as its superior performance over existing methods. In summary, we make three-fold contributions as follows:

- We propose DocMAE, a self-supervised learning-based framework for document image rectification.
- We propose a large-scale dataset based on the rendering techniques for self-supervised representation learning.
- We conduct extensive experiments to verify the merits of our method and report the state-of-the-art performance.

II. RELATED WORK

There are mainly two technical routes to address document image rectification, including (a) rectification based on 3D reconstruction, and (b) rectification based on low-level features. We discuss them separately in the following.

A. Rectification Based on 3D Reconstruction

In order to rectify document images, some traditional methods take advantage of auxiliary equipment to reconstruct the 3D shape of the deformed documents and then flatten the reconstructed surface to correct the distortions. Brown and Seales [4] utilize a light projector to gain the 3D representation of the document shape and then flatten the page through a spring-mass particle system. Zhang et al. [5] fulfill restoration based on physical modeling techniques with the help of a laser scanner. Meng et al. [6] project two structured beams illuminating the document page to recover two spatial curves of the page surface. In comparison, some other methods exploit multi-view images for 3D shape reconstruction. Among them, Koo et al. [7] calculate the corresponding points between two document images by SIFT to resolve the unfolded surface. You et al. [8] present a method based on a ridge-aware 3D reconstruction technique. Tan et al. [20] employ the shading technique to acquire shape for distortion rectification. Das et al. [9] build a 3D shape model with the help of the convolutional neural network. However, no matter whether using auxiliary equipment or taking advantage of multi-view images, these

methods cannot be used in common situations, resulting in the limitation of their usability.

B. Rectification Based on Low-level Features

The low-level features of an image also contain informative cues for geometric distortion rectification. In previous work, many algorithms focus on how to restore the curved text lines straight. For example, Lavielle et al. [21] model the detected text lines as cubic B-splines. While Mischke and Luther et al. [22] utilize polynomial approximation to model it. However, these methods rely more on hand-craft settings and human prior knowledge. The neural network is introduced to solve this task by Ma et al. [10]. They utilize a stacked UNet to directly regress the pixel-wise displacement. Li et al. [11] stitch the displacement field of the image patches to unwrap the image. Xie et al. [12] adopt a fully convolutional network to evaluate pixel-wise displacement. FDRNet [23] transforms the image to the Fourier space to extract structural representations.

III. APPROACH

In this section, we present DocMAE, a novel framework for the geometric rectification of document images. Fig. 1 shows the framework of our method. DocMAE consists of two stages, including: (1) a distortion-aware pre-training stage that reconstructs the randomly masked patches, and (2) a rectification fine-tuning stage that transfers the learned representations for estimating the distortion rectification.

A. Self-supervised Pre-training

In a geometrically distorted document image, the document structure information is reflected by its edges, text lines, and illumination variations, which provides rich cues for distortion rectification. To obtain the structure representation in a convenient way, our DocMAE framework introduces a distortion-aware self-supervised pre-training stage, free of hardware requirements or human supervision.

Background Removal. Due to the diversity of the document image background, the reconstruction of them cannot help the learning of the structure information, different from the reconstruction of text lines and document boundaries. Therefore, to obtain the meaningful features for rectification, we remove the background of the input image $I_d \in \mathbb{R}^{H \times W \times 3}$ during the pre-training stage. Specifically, a lightweight semantic segmentation network [24] is trained to predict the mask $M \in \mathbb{R}^{H \times W \times 1}$ of the foreground document. Then, the noisy background is removed by pixel-wise multiplication along the channel dimension between image I_d and mask M .

Masking. Following ViT [25], we first divide the background-excluded document image $I_e \in \mathbb{R}^{H \times W \times 3}$ into a sequence of 2D patches $x_p \in \mathbb{R}^{N \times (P^2 \cdot 3)}$, where H and W represent the height and width of the document image I_d , P represents the patch size, and $N = HW/P^2$ denotes the number of patches. Then, we randomly mask the N patches x_p with a ratio R .

Distortion Encoder. The distortion encoder extracts the features of the input image I_e . We only process the visible

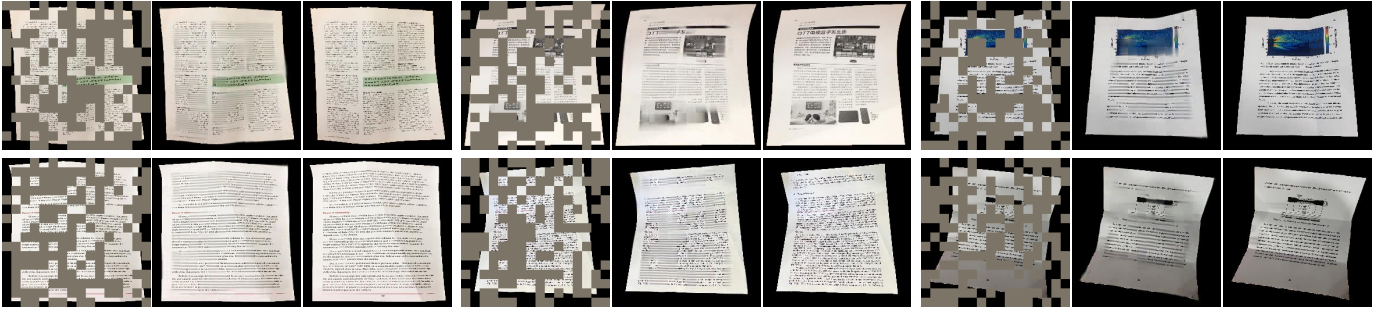


Fig. 2. Example results of real document images. For each triplet, we show the mask image (left), our reconstruction (middle), and the ground truth (right). The masking ratio is set as 50% here.

patches $\mathbf{x}_v \in \mathbb{R}^{N_v \times (P^2 \cdot 3)}$, where $N_v = N \times (1 - R)$ denotes the number of patches. Then, these patches are flattened and mapped to D dimension with a linear projection. The output is the patch embeddings $\mathbf{E}_o \in \mathbb{R}^{N_v \times D}$. Here, we set $D = 512$. To maintain the positional information, positional embeddings $\mathbf{E}_p \in \mathbb{R}^{N_v \times D}$ (the sine-cosine version) are included and bonded with the patch embeddings \mathbf{E}_o . Then, the output passes through K_1 transformer blocks [25] to output encoded visible patches $\mathbf{E}_e \in \mathbb{R}^{N_v \times D}$.

Reconstruction Decoder. The learnable mask tokens $\mathbf{E}_m \in \mathbb{R}^{N_m \times D}$ are zero-initialized and concatenated with encoded visible patches \mathbf{E}_e , where $N_m = N \times R$ is the number of masked patches. Then we add positional embeddings $\mathbf{E}'_p \in \mathbb{R}^{N \times D}$ to all tokens, to help mask tokens gain the information about their locations in the image. The obtained embeddings $\mathbf{E}_d \in \mathbb{R}^{N \times D}$ are then fed into another K_2 transformer blocks [25]. Finally, we employ a linear projection to project the output channels D to the pixel number in each patch, *i.e.*, $P^2 \times 3$. The output $\mathbf{x}_f \in \mathbb{R}^{N \times (P^2 \cdot 3)}$ is reshaped to form the reconstructed image $\mathbf{I}_r \in \mathbb{R}^{H \times W \times 3}$.

Loss Function. The training loss is defined as the L_2 distance between the reconstructed image \mathbf{I}_r and the input background-excluded image \mathbf{I}_e on the masked patches,

$$\mathcal{L}_{pre} = \frac{1}{n} \sum_{i=1}^n (y_i - \hat{y}_i)^2, \quad (1)$$

where y_i denotes the pixel value of the background-excluded image \mathbf{I}_e , \hat{y}_i represents the pixel value of the reconstructed image \mathbf{I}_r , and n denotes the number of reconstructed pixels.

B. Fine-tuning for Rectification

In this section, we transfer the learned representations for downstream distortion rectification. As shown in Fig. 1, a rectification decoder is cascaded to the pre-trained encoder and outputs the rectified image, described next.

Feature Extraction. Given an input image $\mathbf{I}_d \in \mathbb{R}^{H \times W \times 3}$, we first remove its noisy background as the pre-training stage, to make the rectification network focus on the distortion rectification without localizing the document first. Then, the obtained background-excluded document image $\mathbf{I}_e \in \mathbb{R}^{H \times W \times 3}$ is divided into multiple patches, embedded into tokens, and

fed into the pre-trained distortion encoder for representation extraction. Next, we fed the obtained representations into another rectification decoder with K_2 transformer blocks [25]. The output feature $\mathbf{E}_f \in \mathbb{R}^{N \times D}$ is taken as the input of the following flow prediction head.

Flow Prediction. We first reshape the feature $\mathbf{E}_f \in \mathbb{R}^{N \times D}$ to $\mathbf{f}_s \in \mathbb{R}^{\frac{H}{P} \times \frac{W}{P} \times 2}$. Then, we upsample the $\frac{1}{P}$ scale warping flow \mathbf{f}_s to full-scale one $\mathbf{f} \in \mathbb{R}^{H \times W \times 2}$ using a learnable upsample module [13], [26]. Note that \mathbf{f} is a flow field that describes the deformation from the distorted image to the distortion-free one. Given the predicted warping flow $\mathbf{f} \in \mathbb{R}^{H \times W \times 2}$, we resample the pixels from the background-excluded image \mathbf{I}_e to generate the rectified one $\mathbf{I}_c \in \mathbb{R}^{H \times W \times 3}$ as follows,

$$\mathbf{I}_c(u, v) = \mathbf{I}_e(\mathbf{f}_u(u, v), \mathbf{f}_v(u, v)), \quad (2)$$

where (u, v) is the integer pixel coordinate in rectified image, \mathbf{f}_u and \mathbf{f}_v represent the two channel of warping flow \mathbf{f} , and $(\mathbf{f}_u(u, v), \mathbf{f}_v(u, v))$ is the projected coordinate in \mathbf{I}_e .

Loss Function. During the fine-tuning stage, the model is optimized with the training objective as follows,

$$\mathcal{L}_{ft} = \frac{1}{n} \sum_{i=1}^n |y_i - y'_i|, \quad (3)$$

where y_i and y'_i are the coordinates in predicted flow \mathbf{f} and ground truth \mathbf{f}_{gt} , and n denotes the number of pixels in \mathbf{f} .

IV. EXPERIMENT

A. Dataset

Doc3D. Doc3D dataset [15] consists of 100k distorted document images created by real document data with rendering software. It is the largest dataset to date in the field. In this work, we take the Doc3D dataset for training in our approach.

LDIR. To perform self-supervised learning on document images, we propose LDIR, a large-scale synthetic dataset for document image rectification. We utilize 3D rendering software to simulate real-world document textures, lighting conditions, backgrounds, and distortions, which ensures the quality of LDIR. It contains 200k distorted document images. The distorted document images are rendered through real document data in our daily life, such as books and magazines. Our experiments reveal the high quality of LDIR that indeed

improves the rectification performance based on self-supervised learning.

DocUNet benchmark. DocUNet benchmark dataset [10] is a widely-used dataset for the evaluation of rectification algorithms. It contains 130 real-world distorted document images and their scanned ground truth.

B. Setup

We use all the images of LDIR dataset for pre-training and all the images of Doc3D dataset [15] for fine-tuning. The image size (H, W) is (288,288) and the patch size P is 16. During the pre-training stage and fine-tuning stage, the latent vector size D of the encoder and decoder is both 512. The layer number K_1 and K_2 are set as 6 and 4, respectively.

We use the Adam optimizer and one-cycle learning rate policy with a maximum value of 10^{-4} . Both stages are trained for 65 epochs with a batch size of 64. Two NVIDIA GeForce RTX 1080Ti GPUs are employed to train the network.

C. Evaluation Metrics

We discuss the evaluation scheme mainly in two fields: pixel alignment and Optical Character Recognition (OCR) accuracy. Specifically, for pixel alignment, Local Distortion (LD) and Multi-Scale Structural SIMilarity (MS-SSIM) are recommended to evaluate the restoration performance as previous works [10], [12], [15] suggest. In terms of OCR, Edit Distance (ED) and Character Error Rate (CER) are used to evaluate the performance on text recognition, following [10], [15].

Local Distortion. Local Distortion (LD) [8] calculates the average deformation of each pixel and represents the mean displacement error according to the SIFT flow $(\Delta x, \Delta y)$ [27] from the ground-truth scanned image to the rectified one.

MS-SSIM. The Multi-Scale Structural SIMilarity (MS-SSIM) calculates the multi-scale image similarity between the ground-truth scanned image to the rectified one. We follow the weights setting of works [10], [12], [15].

ED and CER. Edit Distance (ED) measures the differences between two strings, based on the minimal number of operations required to change one string into the target one. It involves three types of operations, including deletions (d), insertions (i), and substitutions (s). Furthermore, Character Error Rate (CER) can be computed: $(d + i + s) / N_s$, where N_s is the total number of the target string.

D. Comparison with State-of-the-art Methods

We evaluate the performance of DocMAE on the DocUNet Benchmark dataset [10] by quantitative and qualitative evaluation. Table I shows the comparisons of our DocMAE with the existing state-of-the-art learning-based methods [10]–[12], [15], [23], [28], [29] on distortion metrics, including distortion rectification and OCR accuracy.

As it can be seen in Fig. 3, DocMAE achieves excellent qualitative rectification. Compared with other learning-based methods, the rectified images of DocMAE show less distortion and the corrected text lines are more straight.

TABLE I
QUANTITATIVE COMPARISONS OF THE EXISTING LEARNING-BASED METHODS IN TERMS OF DISTORTION METRICS, OCR ACCURACY, AND IMAGE SIMILARITY ON THE DOCUNET BENCHMARK DATASET. “↑” INDICATES THE HIGHER THE BETTER, WHILE “↓” MEANS THE OPPOSITE.

Methods	Venue	LD ↓	ED ↓	CER ↓	MS-SSIM ↑
Distorted Images	-	20.51	2111.56	0.54	0.25
DocUNet [10]	<i>CVPR'18</i>	14.19	1933.66	0.46	0.41
DocProj [11]	<i>TOG'19</i>	18.01	1712.48	0.43	0.29
DewarpNet [15]	<i>ICCV'19</i>	8.39	885.90	0.24	0.47
FCN-based [12]	<i>DAS'20</i>	7.84	1792.60	0.42	0.45
PWUNet [28]	<i>ICCV'21</i>	8.64	1069.28	0.27	0.49
DDCP [29]	<i>ICDAR'21</i>	8.99	1442.84	0.36	0.47
FDRNet [23]	<i>CVPR'22</i>	8.21	829.78	0.21	0.54
DocMAE (Ours)	-	7.63	801.52	0.20	0.50

TABLE II
ABLATIONS EXPERIMENTS ABOUT THE PRE-TRAINING STAGE FOR REPRESENTATION LEARNING. WITH THE LEARNED REPRESENTATIONS, THE RECTIFICATION PERFORMANCE IMPROVES SIGNIFICANTLY.

Methods	LD ↓	ED ↓	CER ↓	MS-SSIM ↑
w/o pre-training	8.69	854.84	0.23	0.48
w/ pre-training	7.63	801.52	0.20	0.50

E. Ablation Studies

In this section, we conduct ablations to verify the effectiveness of each component in DocMAE, including the self-supervised pre-training, the masking strategy, the way of fine-tuning, and the dataset for pre-training.

Self-supervised Pre-training. The key idea of DocMAE is the self-supervised representation learning strategy for document images. We study the impact of self-supervised learning strategy on the learned representations in Table II. As we can see, self-supervised representation learning significantly boosts the rectification performance. This can be attributed to the representation learning of the structural cues in document images to improve the rectification. Furthermore, as shown in Fig. 2, we show some cases of the reconstructed results using the pre-trained model. The document boundaries and text lines are well-reconstructed. Note that here our goal is not to reconstruct the fine-grained text lines, but to capture their layout caused by perspective and paper distortions.

Masking Ratio. The masking ratio affects the difficulty of self-supervised learning. Therefore, we initialize the pre-training network with different mask ratios. As the result shown in Table III, DocMAE achieves the best performance with a 75% mask ratio. With a higher mask ratio, more details of the document like edges and text lines are missing, which makes the network struggle to extract high-level structural representations. In contrast, with a lower mask ratio, the task is relatively easy for the network to learn effective representations.

Fine-tuning Way. Table IV studies the impact of fine-tuning way on performance. By default, during the fine-tuning stage, we update the weights of the whole model for rectification. Then, we fixed the pre-trained encoder and only fine-tune the



Fig. 3. Qualitative comparison on DocUNet benchmark dataset [10]. Note that such images are real-world document images. Our DocMAE can effectively rectify such images and show less distortion compared with other learning-based methods.

TABLE III

ABLATION EXPERIMENTS ABOUT MASKING RATIO IN THE PRE-TRAINING STAGE. 75% PRODUCES THE BEST PERFORMANCE.

Masking Ratio	LD ↓	ED ↓	CER ↓	MS-SSIM ↑
60%	7.88	808.35	0.20	0.50
75%	7.63	801.52	0.20	0.50
90%	8.21	933.52	0.22	0.49

TABLE IV

ABLATION EXPERIMENTS ABOUT FINE-TUNING WAY. FINE-TUNING THE WHOLE MODEL WORKS BETTER.

Settings	LD ↓	ED ↓	CER ↓	MS-SSIM ↑
freezing the encoder	8.56	1011.64	0.25	0.49
fine-tuning the whole model	7.63	801.52	0.20	0.50

rectification decoder. As we can see, our default fine-tuning way produces much better performance.

Datasets for Pre-training. We ablate the dataset used for pre-training. We use two different datasets separately: the Doc3D dataset [15] and our LDIR dataset. As shown in Table V, the network pre-trained on our LDIR dataset performs much better. We attribute this performance gain to the use of the extra data and the quality of our LDIR dataset.

V. CONCLUSION

In this work, we present DocMAE, a self-supervised framework for document image rectification. The key idea is to capture the structural cues in document images and leverage it for rectification. Technically, we first mask random patches of the background-excluded document images and then reconstruct the missing pixels. In our implementation,

TABLE V

ABLATION EXPERIMENTS ABOUT THE DATASET USED FOR PRE-TRAINING. THE LDIR DATASET HELPS GAIN MORE PRIOR KNOWLEDGE COMPARED WITH THE Doc3D DATASET [15].

Dataset	LD ↓	ED ↓	CER ↓	MS-SSIM ↑
Doc3D	8.05	891.76	0.22	0.49
LDIR	7.63	801.52	0.20	0.50

we collect a large-scale dataset named LDIR based on the rendering techniques. Extensive experiments are conducted, and the results demonstrate the effectiveness of the learned representations as well as the superior rectification performance.

REFERENCES

- [1] Albert Parra Pozo, Andrew W Haddad, Mireille Boutin, and Edward J Delp, "A method for translating printed documents using a hand-held device," in *ICME*, 2011, pp. 1–6.
- [2] Xingjiao Wu, Ziling Hu, Xiangcheng Du, Jing Yang, and Liang He, "Document layout analysis via dynamic residual feature fusion," in *ICME*, 2021, pp. 1–6.
- [3] Zhi Yang, Jun Xuan, Qing Liu, and Aihua Mao, "Modality-specific multimodal global enhanced network for text-based visual question answering," in *ICME*, 2022, pp. 1–6.
- [4] Michael S Brown and W Brent Seales, "Document restoration using 3D shape: a general deskewing algorithm for arbitrarily warped documents," in *ICCV*, 2001, vol. 2, pp. 367–374.
- [5] Li Zhang, Yu Zhang, and Chew Tan, "An improved physically-based method for geometric restoration of distorted document images," *TPAMI*, vol. 30, no. 4, pp. 728–734, 2008.
- [6] Gaofeng Meng, Ying Wang, Shenquan Qu, Shiming Xiang, and Chunhong Pan, "Active flattening of curved document images via two structured beams," in *CVPR*, 2014, pp. 3890–3897.
- [7] Hyung Il Koo, Jinho Kim, and Nam Ik Cho, "Composition of a dewarped and enhanced document image from two view images," *TIP*, vol. 18, no. 7, pp. 1551–1562, 2009.
- [8] Shaodi You, Yasuyuki Matsushita, Sudipta Sinha, Yusuke Bou, and Katsushi Ikeuchi, "Multiview rectification of folded documents," *TPAMI*, vol. 40, no. 2, pp. 505–511, 2017.

- [9] Sagnik Das, Gaurav Mishra, Akshay Sudharshana, and Roy Shilkrot, "The common fold: utilizing the four-fold to dewarp printed documents from a single image," in *DocEng*, 2017, pp. 125–128.
- [10] Ke Ma, Zhixin Shu, Xue Bai, Jue Wang, and Dimitris Samaras, "DocUNet: Document image unwarping via a stacked u-net," in *CVPR*, 2018, pp. 4700–4709.
- [11] Xiaoyu Li, Bo Zhang, Jing Liao, and Pedro V Sander, "Document rectification and illumination correction using a patch-based CNN," *ACM TOG*, vol. 38, no. 6, pp. 1–11, 2019.
- [12] Guowang Xie, Fei Yin, Xuyao Zhang, and Chenglin Liu, "Dewarping document image by displacement flow estimation with fully convolutional network," in *DAS*, 2020, pp. 131–144.
- [13] Hao Feng, Yuechen Wang, Wengang Zhou, Jiajun Deng, and Houqiang Li, "DocTr: Document image transformer for geometric unwarping and illumination correction," in *ACM MM*, 2021, pp. 273–281.
- [14] Hao Feng, Wengang Zhou, Jiajun Deng, Yuechen Wang, and Houqiang Li, "Geometric representation learning for document image rectification," in *ECCV*, 2022, pp. 475–492.
- [15] Sagnik Das, Ke Ma, Zhixin Shu, Dimitris Samaras, and Roy Shilkrot, "DewarpNet: Single-image document unwarping with stacked 3D and 2D regression networks," in *ICCV*, 2019, pp. 131–140.
- [16] Michael S Brown, Mingxuan Sun, Ruigang Yang, Lin Yun, and W Brent Seales, "Restoring 2D content from distorted documents," *TPAMI*, vol. 29, no. 11, pp. 1904–1916, 2007.
- [17] Atsushi Yamashita and et al. Kawarago, Atsushi, "Shape reconstruction and image restoration for non-flat surfaces of documents with a stereo vision system," in *ICPR*, 2004, vol. 1, pp. 482–485.
- [18] Olaf Ronneberger, Philipp Fischer, and Thomas Brox, "U-Net: Convolutional networks for biomedical image segmentation," in *MICCAI*, 2015, pp. 234–241.
- [19] Kaiming He, Xinlei Chen, Saining Xie, Yanghao Li, Piotr Dollár, and Ross Girshick, "Masked autoencoders are scalable vision learners," in *CVPR*, 2022.
- [20] Chew Lim Tan, Li Zhang, Zheng Zhang, and Tao Xia, "Restoring warped document images through 3D shape modeling," *TPAMI*, vol. 28, no. 2, pp. 195–208, 2005.
- [21] Olivier Laviolle, X Molines, Franck Angella, and Pierre Baylou, "Active contours network to straighten distorted text lines," in *ICIP*, 2001, vol. 3, pp. 748–751.
- [22] Lothar Mischke and Wolfram Luther, "Document image de-warping based on detection of distorted text lines," in *ICIAP*, 2005, pp. 1068–1075.
- [23] Chuhui Xue, Zichen Tian, Fangneng Zhan, Shijian Lu, and Song Bai, "Fourier document restoration for robust document dewarping and recognition," in *CVPR*, 2022, pp. 4573–4582.
- [24] Xuebin Qin, Zichen Zhang, Chenyang Huang, Masood Dehghan, Osmar R Zaiane, and Martin Jagersand, "U2-net: Going deeper with nested u-structure for salient object detection," *PR*, vol. 106, pp. 107404, 2020.
- [25] Alexey Dosovitskiy, Lucas Beyer, Alexander Kolesnikov, Dirk Weissenborn, Xiaohua Zhai, Thomas Unterthiner, Mostafa Dehghani, Matthias Minderer, Georg Heigold, Sylvain Gelly, et al., "An image is worth 16x16 words: Transformers for image recognition at scale," in *ICLR*, 2020.
- [26] Hao Feng, Wengang Zhou, Jiajun Deng, Qi Tian, and Houqiang Li, "DocScanner: Robust document image rectification with progressive learning," *arXiv preprint arXiv:2110.14968*, 2023.
- [27] Ce Liu, Jenny Yuen, and Antonio Torralba, "Sift flow: Dense correspondence across scenes and its applications," *TPAMI*, vol. 33, no. 5, pp. 978–994, 2010.
- [28] Sagnik Das, Kunwar Yashraj Singh, Jon Wu, Erhan Bas, Vijay Mahadevan, Rahul Bhotika, and Dimitris Samaras, "End-to-end piece-wise unwarping of document images," in *ICCV*, 2021, pp. 4268–4277.
- [29] Guo-Wang Xie, Fei Yin, Xu-Yao Zhang, and Cheng-Lin Liu, "Document dewarping with control points," in *ICDAR*, 2021, pp. 466–480.